

and further, that CT results do not effectively predict clinical symptoms. Magnetic resonance imaging (MRI) characterized by high multiparameter sensitivity enables a reliable basis for early detection and diagnosis of mTBI (Toth, 2015). Developing an MRI-based analytical method for mTBI mechanism and prognostic evaluation has important practical significance for effectively reducing TBI disability rate and medical cost (Aquino et al., 2015). MRI can detect intracranial hemorrhages and microhemorrhages after mTBI (Huang et al., 2015), but is seldom used to measure changes in cerebral blood flow (CBF). Indeed, it remains unclear how CBF alters after mTBI.

CBF reflects blood flow perfusion in the brain, and is strongly associated with brain function. Abnormal CBF is the main symptom and diagnostic evidence of stroke, epilepsy, cerebral infarction, and brain tumor (Grade et al., 2015). There are many methods to measure CBF. Dynamic susceptibility contrast-enhanced MRI using the paramagnetic contrast agent, gadolinium diethyl triamine, can be used, but is not suitable for patients in renal failure (Ostergaard et al., 1996; Smith, 2012). Position emission tomography and single-photon emission CT use radioactive tracers, so are not suitable for children and patients requiring long-term follow-up (Ott, 1994). Finally, arterial spin labeling can effectively measure CBF in a normal person, as shown previously (Sharp et al., 2011) and corroborated by position emission tomography results (Ostergaard et al., 1996). Pulsed arterial spin labeling is extensively used at present, and characterized by high image quality, low hardware requirements, simple operation, high mark-power, and small power deposition. Moreover, it nondestructively detects changes in blood flow perfusion in the brain (Wu et al., 2007). We designed this study to dynamically observe CBF changes using pulsed arterial spin labeling in mTBI patients compared with normal subjects.

Subjects and Methods

Subjects

TBI patients were collected from the Department of Emergency and Department of Neurosurgery of the Second Xiangya Hospital, Central South University of China from January 2013 to December 2014.

Inclusion criteria

(1) Meet one or more of the following symptoms: confusion of consciousness or inability to discern direction, loss of consciousness for < 30 minutes, time of coma < 24 hours, transient epilepsy, partial nerve damage, but does not require surgery; (2) acute confusion, a Glasgow Coma Scale (GCS) score of 13–15; (3) complete clinical data; (4) no severe cardiopulmonary disease, can tolerate MRI for 30 minutes; and (5) no MRI contraindications and claustrophobia (Palacios et al., 2013).

Exclusion criteria

(1) A history of cerebral trauma; (2) history of space-occupying lesion, vascular malformation, venous sinus throm-

bosis, or other central nervous system disease; (3) history of drug abuse, alcoholism, and mental illness; (4) open traumatic brain injury; and (5) MRI contraindications.

According to the inclusion and exclusion criteria, 20 mTBI patients (13 males and 7 females) aged 18–40 years (mean 39.05 ± 5.56 years) were recruited. There were seven cases of traffic accident injury, five cases of high-fall injury, six cases of fall-related injury, and two cases of combat injury. All patients were right-handed. All subjects received MRI at the acute stage (within 72 hours), subacute stage (3 days–3 weeks), and chronic stage (more than 3 months) after injury.

Twenty healthy subjects were recruited by advertisement. Their sex, age, and educational level were matched with subjects in the mTBI group. The exclusion criteria were identical to those in the mTBI group. There were 13 males and 7 females, aged 19–42 years (mean 38.65 ± 6.54 years). All healthy subjects were right-handed.

All subjects and their family members were informed about the purpose and methods of the study, and provided written, informed consent. The protocols were approved by the Ethics Committee of the Second Xiangya Hospital, Central South University of China (Approval No. 2012 227).

MRI and pulsed arterial spin labeling

MRI and pulsed arterial spin labeling scanning were performed using a 3.0 T MRI scanner (Siemens Medical Solutions, Erlangen, Germany), with a 16-channel phased array coil. After removal of metal objects, subjects were made familiar with the environment and experimental procedures. The subjects lay in the supine position. They were breathing smoothly, and could not move their heads. The long axis of the body was parallel to the long axis of the main field. The head was located in the center of the coil. The sagittal position cursor was placed in the center of the face. Their heads were fixed with a sponge mat. Their ears were tightly plugged with ear plugs. If the subjects did not feel uncomfortable, scanning began. MRI was terminated if the subjects experienced any discomfort or an unexpected situation.

Routine MRI sequence: axial, coronal, and sagittal images; T2 weighted image (T2WI) turbo spin-echo (TSE) sequence (repetition time 4,050 ms, echo time 105 ms), T2 fluid attenuation inversion recovery (FLAIR) sequence (repetition time 7,000 ms, echo time 120 ms, inversion recovery 2,000 ms), and T1 weighted image (T1WI) fast spin echo (FSE) sequence (repetition time 450 ms, echo time 15 ms, field of view $190 \text{ mm} \times 230 \text{ mm}$, matrix 240×320 , slice thickness 5.0 mm, spacing 0.5 mm, number of slices 25).

Pulsed arterial spin labeling sequence: functional images were collected (repetition time 2,500 ms, echo time 11 ms, inversion time 1: 700 ms, inversion time 2: 1,800 ms, slice thickness 8 mm, slices 11, bandwidth 2,232 Hz/PX, flip angle 90° , matrix 64×64 , field of view $256 \text{ mm} \times 256 \text{ mm}$). In total, 91 frame images were collected from each subject.

3D scanning was followed by a magnetization prepared rapid acquisition gradient echo sequence (repetition time 1,900 ms, echo time 2.81 ms, inversion time 900 ms, flip angle 9° , slice thickness 1 mm, bandwidth 260 Hz/PX, matrix $256 \times$

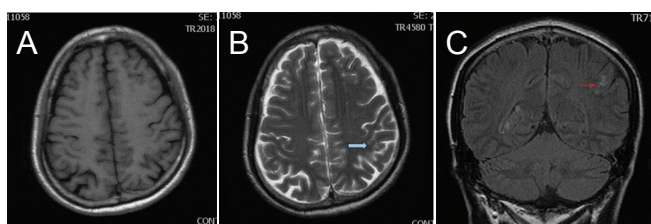


Figure 1 Routine magnetic resonance imaging results from a 57-year-old male patient after mild traumatic brain injury for 3 days. (A) T1WI did not reveal evident lesions with no abnormal signal detected. (B) T2WI demonstrated patchy lesions with high signal intensity on the left cortex of the parietal lobe (arrow). (C) T2 FLAIR sequence exhibited remarkably patchy lesions with high signal intensity on the left cortex of the parietal lobe (arrow). T1WI: T1 weighted image; T2WI: T2 weighted image; FLAIR: fluid-attenuated inversion recovery.

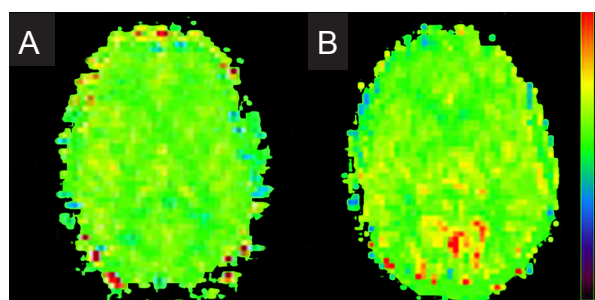


Figure 2 Perfusion image of CBF of magnetic resonance imaging pulsed arterial spin labeling.

(A) In the normal control group, blood flow was greater, and CBF value was higher, in the occipital, frontal, and parietal cortices. Additionally, blood flow was reduced in the white matter. (B) In patients with cerebral hemorrhage, perfusion was low, and CBF reduced, in bilateral frontal lobes. Red color: Abundant blood flow; purple color: low blood flow; CBF: cerebral blood flow.

Table 1 CBF (mL/min/100 g) distribution in the brain of normal controls and mTBI patients

Group	Occipital lobe	Parietal lobe	Temporal lobe	Insula	Limbic lobe	Subcutaneous region	Central lobe	Frontal lobe	White matter	Gray matter	Whole brain
Control	55.0±3.9	48.3±3.6	45.0±3.6	43.8±3.7	40.2±3.7	34.6±3.6	38.5±3.5	34.3±3.4	29.2±4.2	45.5±2.2	34.0±3.3
mTBI 1 st	39.7±2.5*	34.2±3.0*	30.0±2.3*	42.5±2.8	24.8±2.2*	20.4±2.1*	23.2±2.1*	20.5±2.0*	17.2±2.8*	32.4±3.3*	19.7±2.5*
mTBI 2 nd	48.9±3.7*	42.5±2.8*	40.0±2.8*	43.6±3.8	34.5±2.3*	31.7±3.6*	33.2±1.8*	31.5±3.5*	24.3±3.2*	37.8±2.5*	28.9±3.7*
mTBI 3 rd	54.5±4.0	47.8±3.4	44.3±3.1*	42.8±3.5	39.4±4.0*	34.5±3.6	38.1±3.4	34.4±3.4	28.6±3.9	44.8±1.7	32.6±3.1

CBF was compared between normal controls ($n = 20$) and mTBI patients at the acute, subacute, and chronic stages ($n = 20$). mTBI 1st: acute stage; mTBI 2nd: subacute stage; mTBI 3rd: chronic stage. Data are expressed as the mean ± SD. Between-group differences were assessed by Student's *t*-test (for normally distributed continuous variables) and Mann-Whitney *U* test (non-normal continuous variables). * $P < 0.05$, vs. control group. CBF: Cerebral blood flow; mTBI: mild traumatic brain injury.

256, field of view 256 mm × 256 mm). In total, 176 layers of sagittal images were collected from all over the brain.

Data processing of resting state pulsed arterial spin labeling

Data from 3D structural images and pulsed arterial spin labeling functional images were processed using the Matlab2009 (Matrix Laboratory, Mathworks Company, Natick, MA, USA) data processing platform and SPM8 Toolbox (Statistical Parametric Mapping, <http://www.fil.ion.ucl.ac.uk/spm/>) (Friston et al., 1994). The following steps were performed: (1) image format conversion; (2) removal of images in the previous five time points (due to magnetic field inhomogeneity, nervous subjects, head movement, or unstable data); (3) head correction: this study excluded subjects whose head movement was > 1 mm and angle of rotation > 1°; (4) spatial registration; (5) spatial smoothing; (6) calculation of CBF: after calculating perfusion images, mean CBF was calculated in each subject; (7) space standardization: SPM8 software uses the International Consortium for Brain Mapping 152 human brain atlas, formulated by the Montreal Neurological Institute, Montreal, Canada; (8) correction for partial-volume effects; (9) selection of regions of interest: using Automated Anatomical Labeling (Friston et al., 1994), the brain was divided into 90 regions in eight brain regions, including central region, frontal lobe, occipital lobe, parietal lobe, temporal lobe, insula, limbic lobe, and cortex. Perfu-

sion values for these 90 brain regions were calculated, and from these a mean value calculated. Additionally, perfusion values were calculated in 11 brain regions including whole brain, gray matter, and white matter.

Statistical analysis

Images after perfusion were analyzed in regions of interest for all subjects. CBF values were measured in 11 brain regions of interest. Data normality was assessed by the Kolmogorov-Smirnov test. Results for continuous variables are presented as the mean ± SD. Between-group differences were assessed by Student's *t*-test (for normally distributed continuous variables) and Mann-Whitney *U* test (non-normal continuous variables). All statistical comparisons were performed using SPSS software 18.0 (SPSS, Chicago, IL, USA). *P* values < 0.05 were considered statistically significant.

Results

Routine MRI results in mTBI patients

No visible abnormal signal was detected in 20 normal controls. Moreover, the ventricular system size and morphology were normal, with a narrow cerebral fissure and cistern, and central midline. Of the 20 mTBI patients, 15 had normal MRI results, with no abnormal signal found. T1 and T2 sequences showed abnormal signal in three patients. T2-FLAIR sequence demonstrated lesions with high signal intensity in the gray and white matter of five patients (Figure 1).

MRI pulsed arterial spin labeling sequence results in mTBI patients

CBF was decreased in the occipital lobe, parietal lobe, subcutaneous area, central area, and frontal lobe of mTBI patients after injury ($P < 0.05$). This was restored 3 months later ($P > 0.05$). CBF was diminished in the temporal and limbic lobes at the acute stage and restored 3 months later, with significant differences detected between patients and normal controls ($P < 0.05$). No significant difference in CBF in insula was found at the acute stage, 3 days–3 weeks, and 3 months. CBF was maximal in the gray matter, followed by the whole brain, and then minimal in the white matter. CBF was reduced in the gray and white matter by mTBI. Moreover, it was reduced in the whole brain at the acute and subacute stages, and then restored at the chronic stage, at approximately 3 months (Table 1). Blood flow was greatest in the occipital, frontal, and parietal cortices. CBF was highest in the normal control group. Blood flow was lower in the white matter, and decreased at the site of injury (Figure 2).

Discussion

Previous studies have commonly used gradient echo and susceptibility weighted imaging to detect bleeding and microhemorrhages. Susceptibility weighted imaging is very sensitive to microhemorrhagic foci caused by TBI (Liu et al., 2014; Liu et al., 2015). However, these sequences are limited in detection of blood flow. In this study, we used pulsed arterial spin labeling to dynamically observe changes in CBF after mTBI.

Despite different measurements and selection criteria for regions of interest, CBF is 35–78 mL/min/100 g in gray matter (Petersen et al., 2006). Based on pulsed arterial spin labeling, we found CBF was 45.45 mL/min/100 g in the gray matter of normal controls, which is consistent with a previous study (Petersen et al., 2006). Further, our results confirm low CBF in mTBI patients at the acute and subacute stages, which is restored 3 months later at the chronic stage. Our CBF results are consistent with the studies by Chen et al. (2011), using arterial spin labeling, and Donahue et al. (2006), using position emission tomography. Compared with position emission tomography, pulsed arterial spin labeling is characterized by less hardware requirement, simple operation, high labeling efficiency, and low power deposition.

Additionally, our results show that CBF is higher in gray matter than white matter in normal controls and mTBI patients, while whole brain CBF is between gray and white matter, consistent with metabolic activity in the human brain. Metabolic activity is higher in gray matter nuclei compared with white matter in the central nervous system (Petersen et al., 2010). Blood flow perfusion was greater in the gray matter than white matter. Metabolic activity in whole brain is the integration of gray and white matter activity. Thus, the CBF value in the whole brain is higher than in white matter, but lower than in gray matter. In mTBI patients, CBF changed at the acute and subacute stages in the whole brain, gray matter, and white matter, but was still

higher in gray matter than white matter, in accordance with CBF distribution in normal persons.

We found that CBF basically restored at 3 months after injury in mTBI patients, which suggests strong brain self-regulation. Changes in CBF in the insula were not pronounced. We assumed that as the other brain regions are on the brain surface they would be easily impacted by an external force, and therefore the mechanisms of nervous-humoral regulation and blood flow alteration had begun. Accordingly, the insula is located deep in the brain and protected by the skull and surrounding brain tissue, so CBF changes were not great. We also confirmed that among eight brain regions, no significant difference in CBF was detected in six brain regions (occipital lobe, parietal lobe, insula, subcutaneous area, central area, and frontal lobe) between with mTBI patients and normal controls at 3 months (chronic stage). Only the limbic lobe and temporal lobe showed significant differences, although the reason for this remains unclear. Temporary mTBI increases several times the incidence of cognitive disorders (Walker et al., 2012). TBI also causes the brain to produce pathological changes similar to Alzheimer's disease and drug addiction (Sivanandam and Thakur, 2012), and is a high-risk factor for diseases. We assumed that CBF differences in the limbic lobe and temporal lobe may be one of the causes of mental cognitive impairment caused by mTBI. The main functions of the temporal and limbic lobes are to regulate visceral function, and association with emotional responses and memory activities. If these are not corrected for a long time or corrected incompletely, CBF changes after mTBI may induce functional compensation. If they cannot be completely compensated, CBF changes may lead to mental and cognitive impairment.

There are several limitations to this study. First, the number of cases is rather small and the statistical analyses are preliminary. We recognize that more detailed statistical analysis with a larger number of cases is still needed. Second, we need another method to measure CBF to confirm accuracy of the pulsed arterial spin labeling method. Third, we only analyzed patients with mTBI, and did not measure CBF in patients with moderate and severe cerebral trauma, which may help to understand the mechanism of brain injury.

In summary, pulsed arterial spin labeling can quantitatively and dynamically monitor CBF. CBF is reduced in most brain regions at the acute and subacute stages following mTBI, and restored at the chronic stage. Changes in CBF are not obvious in the insula at these stages. CBF in the limbic lobe at the chronic stage is still lower in patients than in normal controls. Pulsed arterial spin labeling can exert a certain reference effect on assessment and prognosis of traumatic brain injury.

Author contributions: SPP wrote the paper, provided data and ensured the integrity of the data. YNL collected data and wrote the paper. JL conceived and designed this study, and was in charge of paper authorization. ZYW analyzed data. FXT and ZXZ performed statistical analysis. ZSZ and SKZ served as principle investigator. All authors approved the final version

of the paper.

Conflicts of interest: None declared.

Plagiarism check: This paper was screened twice using Cross-Check to verify originality before publication.

Peer review: This paper was double-blinded and stringently reviewed by international expert reviewers.

References

- Aquino C, Woolen S, Steenburg S (2015) Magnetic resonance imaging of traumatic brain injury: a pictorial review. *Emerg Radiol* 22:65-78.
- Chen Y, Wang DJ, Detre JA (2011) Test-retest reliability of arterial spin labeling with common labeling strategies. *J Magn Reson Imaging* 33:940-949.
- Donahue MJ, Lu H, Jones CK, Pekar JJ, van Zijl PC (2006) An account of the discrepancy between MRI and PET cerebral blood flow measures. A high-field MRI investigation. *NMR Biomed* 19:1043-1054.
- Friston KJ, Holmes AP, Worsley KJ, Poline JB, Frith CD, Frackowiak RS (1994) Statistical parametric maps in functional imaging: a general linear approach. *Hum Brain Mapp* 2:189-210.
- Grade M, Hernandez Tamames JA, Pizzini FB, Achten E, Golay X, Smits M (2015) A neuroradiologist's guide to arterial spin labeling MRI in clinical practice. *Neuroradiology* doi:10.1007/s00234-015-1571-z.
- Huang YL, Kuo YS, Tseng YC, Chen DY, Chiu WT, Chen CJ (2015) Susceptibility-weighted MRI in mild traumatic brain injury. *Neurology* 84:580-585.
- Liu J, Kou Z, Tian Y (2014) Diffuse axonal injury after traumatic cerebral microbleeds: an evaluation of imaging techniques. *Neural Regen Res* 9:1222-1230.
- Liu J, Xia S, Hanks R, Wiseman N, Peng C, Zhou S, Haacke EM, Kou Z (2015) Susceptibility weighted imaging and mapping of micro-hemorrhages and major deep veins after traumatic brain injury. *J Neurotrauma* doi:10.1089/neu.2014.3856.
- Ostergaard L, Weisskoff RM, Chesler DA, Gyldensted C, Rosen BR (1996) High resolution measurement of cerebral blood flow using intravascular tracer bolus passages. Part I: Mathematical approach and statistical analysis. *Magn Reson Med* 36:715-725.
- Ott R (1994) PET and SPECT functional imaging. In: *Functional Imaging*, IEE Colloquium on, pp 3/1-3/2. London: IET.
- Palacios EM, Sala-Llonch R, Junque C, Roig T, Tormos JM, Bargallo N, Vendrell P (2013) Resting-state functional magnetic resonance imaging activity and connectivity and cognitive outcome in traumatic brain injury. *JAMA Neurol* 70:845-851.
- Petersen ET, Lim T, Golay X (2006) Model-free arterial spin labeling quantification approach for perfusion MRI. *Magn Reson Med* 55:219-232.
- Petersen ET, Mouridsen K, Golay X, all named co-authors of the QUASAR test-retest study (2010) The QUASAR reproducibility study, Part II: Results from a multi center arterial spin labeling test-retest Study. *NeuroImage* 49:104-113.
- Ruff RL, Riechers RG (2012) Effective treatment of traumatic brain injury: learning from experience. *JAMA* 308:2032-2033.
- Sharp DJ, Beckmann CF, Greenwood R, Kinnunen KM, Bonnelle V, De Boissezon X, Powell JH, Counsell SJ, Patel MC, Leech R (2011) Default mode network functional and structural connectivity after traumatic brain injury. *Brain* 134:2233-2247.
- Sivanandam TM, Thakur MK (2012) Traumatic brain injury: A risk factor for Alzheimer's disease. *Neurosci Biobehav Rev* 36:1376-1381.
- Smith K (2012) Traumatic brain injury: CT scan does not predict outcome of mild traumatic brain injury. *Nat Rev Neurol* 8:474.
- Toth A (2015) Magnetic resonance imaging application in the area of mild and acute traumatic brain injury: implications for diagnostic Markers? In: *Brain Neurotrauma: Molecular, Neuropsychological, and Rehabilitation Aspects* (Kobeissy FH, ed). Boca Raton: CRC Press.
- Ventura RE, Balcer LJ, Galetta SL (2014) The neuro-ophthalmology of head trauma. *Lancet Neurol* 13:1006-1016.
- Walker KR, Kang EL, Whalen MJ, Shen Y, Tesco G (2012) Depletion of GGA1 and GGA3 mediates post-injury elevation of BACE1. *J Neurosci* 32:10423-10437.
- Wu WC, Fernández-Seara M, Detre JA, Wehrli FW, Wang J (2007) A theoretical and experimental investigation of the tagging efficiency of pseudocontinuous arterial spin labeling. *Magn Reson Med* 58:1020-1027.

Copiedited by James R, de Souza M, Yu J, Qiu Y, Li CH, Song LP, Zhao M